

A NEW FAMILY OF ISOCHRONOUS ARCS

G. Guignard and E. T. d'Amico CERN, 1211 Geneva 23, Switzerland

For the Compact Linear Collider (CLIC), the bunch time structure should be preserved in the injection complex especially in the recirculators and after the final bunch compression stage up to the main linac injection point. At the same time because the transverse emittances are so tiny, their growth, essentially by synchrotron radiation, should be kept as slow as possible. In the project several isochronous arcs have been designed numerically to meet these requirements for a particular layout. These designs cannot be easily adapted to different configurations. The purpose of this study is to obtain analytical expressions for a new class of isochronous arcs which can be quickly tailored to special applications. Some of these are presented and they emphasize the small transverse emittance growth achievable even at large injection energy while keeping the arc radius a reasonable value. Because usually the first-order isochronicity is fully cancelled, higher-order contributions are less important than in other designs.

I. INTRODUCTION

In the Compact Linear Collider (CLIC) many considerations (wake-field effects, high luminosity) require that the bunch time structure should be preserved after the last bunch compression stage. This condition in general cannot be fulfilled when the beam passes through a deflecting system because of the difference in length between the individual bits due to the energy spread and to the different initial conditions. The system is called isochronous when it does not change the bunch time structure. It can be proved [1] that in the linear approximation such a system should be nondispersive and such that:

$$\int_{S_1}^{S_2} \frac{D(s)}{\rho(s)} ds = 0 \quad (1)$$

where $D(s)$ is the horizontal dispersion, $\rho(s)$ the radius of curvature and S_1, S_2 are the positions of the beginning and end of the insertion.

The relation (1) shows that contributions to the integral come only from deflecting magnets and off-centred quadrupoles.

Several schemes of isochronous arcs have been developed [2], [3]. They are based on lattices comprising several deflecting magnets where the integral (1) is minimized numerically by the whole arc. The purpose of this study was to investigate analytically isochronous modules with the minimum number of deflecting magnets. The juxtaposition of identical modules allows the building up of a whole family of isochronous arcs depending upon some parameters which can be adjusted to meet special design constraints, such as minimization of the emittance growth due to synchrotron radiation.

It can be proved [1] that the minimum number of deflecting magnets in an isochronous module is three. For reasons of simplicity we have chosen a symmetric module about the mid-plane of the central deflecting magnet.

II. ISOCHRONICITY CONDITION

Let us consider an isochronous insertion with three bending magnets (see Fig. 1) where we neglect for the moment the presence of the magnetic elements assumed to be perfectly centred. To simplify the algebra the bending magnets will be treated as sector magnets of the same length but of different curvature radii ρ_1 and ρ_2 , the deflection angle being respectively ϕ_1 and ϕ_2 .

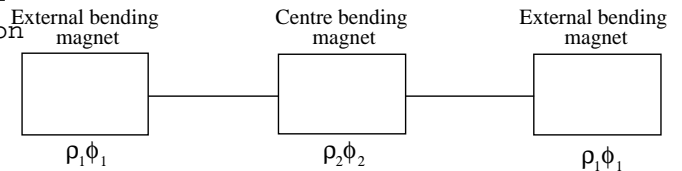


Figure 1: Isochronous insertion bending magnet configuration.

Assuming that the dispersion and its derivative are zero at the entrance of the first magnet, it is easy to show that the isochronicity and symmetry conditions lead to the following expressions for the dispersion and its derivative at the entrance of the centre magnet [4]:

$$\begin{aligned} D_j &= \frac{\epsilon}{\rho_2} D_j^0 \text{ctn}(\phi_2/2) + \frac{1}{\rho_1} \\ D_j^0 &= i \frac{\rho_1}{\rho_2} \frac{3}{2} \phi_1 \sin \phi_1 \end{aligned} \quad (2)$$

III. INSERTION DESIGN

To transport the beam through the insertion as described in Fig. 1, we have to add quadrupoles between the bending magnets. The simplest configuration is FODO, as shown in Fig. 2 where only a half-insertion is shown.

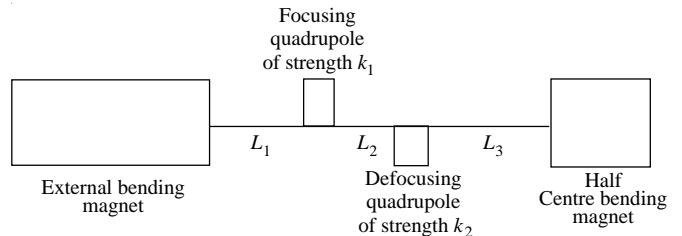


Figure 2: Layout of half isochronous insertion.

The three spaces $L_1; L_2; L_3$ and the two quadrupole strengths $k_1; k_2$ have to be chosen in order for the expressions (2) to be satisfied. After some manipulation of the transfer matrices (see Appendix A of reference [4]) the following expressions for the three drift lengths as functions

Table 1: Permitted ranges of $k_1; k_2; \phi L_3$

| | |
|---|---|
| $k_1 \cdot \text{Min}f_{k_1}^{(1)}; k_{\text{max}} g$ | $\phi_2 < \phi_1; d \text{ and } \phi L_3 > \text{Max}fd; D_j=D_j^0; i; \phi_2 g$ |
| $k_1^{(1)} < k_1 \cdot \text{Min}f_{k_1}^{(2)}; k_{\text{max}} g$ | $\phi_2 > \phi_1; d \text{ and } \text{Max}fd; D_j=D_j^0; i; \phi_2 g < \phi L_3 < \phi L_3^{(1)}$ |
| $k_1^{(1)} < k_1 \cdot \text{Min}f_{k_1}^{(2)}; k_1^{(3)}; k_{\text{max}} g$ | $P \sqrt{k_2} > \text{Max} \frac{\text{acosh}(\text{Max}f_{k_1}^{(2)}/C_2'g)}{L_q}; k_2^{(1)} \text{ and } \text{Max}fd; D_j=D_j^0; \phi L_3^{(2)} g < \phi L_3 < \phi L_3^{(1)}$ |
| $k_1^{(1)} < k_1 < \text{Min}f_{k_1}^{(3)}; k_{\text{max}} g$ | $P \sqrt{k_2} < \frac{\text{acosh}(C_2')}{L_q} \text{ and } \text{Max}fd; D_j=D_j^0; \phi L_3^{(2)} g < \phi L_3 < \phi L_3^{(1)}$ |
| $k_1^{(2)} < k_1 < \text{Min}f_{k_1}^{(3)}; k_{\text{max}} g$ | $P \sqrt{k_2} < \text{Min} k_2^{(1)}; \frac{\text{acosh}(C_2')}{L_q} \text{ and } \text{Max}fd; D_j=D_j^0; \phi L_3^{(2)} g < \phi L_3 < \phi L_3^{(1)}$ |
| $k_1^{(1)} < k_1 < k_{\text{max}}$ | $\phi_2 < \phi_1; d \text{ and } \phi L_3 > \text{Max}fd; D_j=D_j^0; \phi L_3^{(2)} g$ |
| where $k_1^{(1)}; k_1^{(2)}; k_1^{(3)}; k_2^{(1)}$ are the solutions of the following transcendental equations: | |
| $(1+d) \frac{q}{k_1^{(1)}} \tan(L_q k_1^{(1)}) = 1; \quad k_1^{(2)} = \frac{P \sqrt{\cos(L_q k_1^{(2)}(1+2d) + 1) \cos(L_q k_1^{(2)}) + 4d(1+d)}}{2 \sin(L_q k_1^{(2)}d(1+d))}$ $(1+d) \frac{q}{k_1^{(3)}} \sin(L_q k_1^{(3)}); \cos(L_q k_1^{(3)}) = a; \quad k_2^{(1)} \sin(L_q k_2^{(1)}); P \sqrt{k_2^{(1)}} \cosh(L_q k_2^{(1)}); C_2' \sqrt{k_2^{(1)}} = 0$ | |
| and $C_2'; k_2'; k_{\text{max}}; \phi L_3^{(1)}; \phi L_3^{(2)}$, are given by the expressions | |
| $C_2' = \frac{a q_1}{c_1(1+q_1+d)}; k_2' = \frac{h}{d_1 q_1} + \frac{1}{1 + \frac{c_2'}{a c_1}}; k_{\text{max}} = \frac{m}{4L_q^2}; \quad \phi L_3^{(1)} = \frac{b}{d+q_2 i q_1}; \phi_2; \phi L_3^{(2)} = \frac{q_2 c_1}{a q_1 c_2} (1+q_1+d); \phi_2$ | |

of $k_1; k_2$ and of the free parameter $\phi L_3 = L_3; D_j=D_j^0$, this is possible only when the betatron function and its derivative at both ends of such a module are respectively:

$$L_1 = a \frac{C_2 q_1}{C_1 \phi_2} (\phi L_3 + \phi_2); 1 + q_1 \quad f_0 = \frac{P}{1 + m^2} = \frac{1}{m_{21}^2} \text{ and } f_0^0 = 0 \quad (5)$$

$$L_2 = q_1 i \phi_2 + \frac{b}{\phi L_3 + \phi_2}$$

$$L_3 = D_j=D_j^0 + \phi L_3 \quad (3)$$

where

$$1 = \frac{q_1}{c_1} \tan(L_q k_1^{(1)}); \quad a = \frac{1}{\sin(L_q k_1^{(1)})};$$

$$b = \frac{q_2}{c_2} \frac{q_2}{c_2} + \frac{q_1}{a c_1}; \quad q_1 = \frac{C_1}{s_i k_1};$$

$$C_1 = \cos(L_q k_1^{(1)}); \quad S_1 = \sin(L_q k_1^{(1)}); \quad (4)$$

$$C_2 = \cosh(L_q k_2^{(1)}); \quad S_2 = \sinh(L_q k_2^{(1)})$$

L_q being the quadrupole length. Table 1 gives a subset of the ranges of $k_1; k_2; \phi L_3$ for which the three drift lengths are larger than a given value, when

$$\frac{1}{q_1} \cdot \frac{1}{1+d} + \frac{1}{L_q=2+d} :$$

This can be shown to be the case for most of the usual hardware configurations. The full set of conditions may be found in Appendix C of [4].

IV. ARC DESIGN

To build an arc we have to connect as many insertions as are necessary to obtain the desired deflection. To avoid large excursions of the betatron functions, the easiest way is to take advantage of the insertion symmetry and to ensure that the values of the Twiss parameters at both ends of a module composed of an insertion are described above and of a matching section are the same. It is easy to show that

parameters $m_{11} = m_{22}$ and m_{21} are the elements of the transfer matrix for the module. It is very difficult to do without the matching section while satisfying these constraints in both planes. We have preferred to choose a matching section at both ends of the insertion to obtain a module with $|1 - m| < 1$ in both planes. The Twiss parameters at the end of the transfer in an injecting in the arc should then be matched to the values given by the expressions (5). In order to reduce to a minimum the contribution of magnetic errors and the sextupole effects we add the condition that the phase advance over a small number of modules should be an integer multiple of π in both planes.

After some manipulations it is possible to show that the growth of the normalized horizontal emittance ϵ_x is in good approximation inversely proportional to the fourth power of the number of modules required to assemble an arc [4]. The diameter of a full-circle is of course proportional to the number of modules. Clearly a compromise must be found between these two very important design parameters. To find it we have written a simple interactive program as an Excel spreadsheet which permits one to quickly obtain the main features of a 2... arc according to different choices of the number of required modules of the arc, between the radius of curvature of the external and central bending magnets and of the gradients of the two quadrupoles and of the distance ϕL_3 .

V. APPLICATIONS

In each branch of CLIC, two 360-degree arcs are needed to guide the particles in the reverse direction at 3 GeV for the drive beam and the other at 9 GeV for the main beam. These arcs should not perturb the bunch length, which is carefully chosen for optimum performance at the final interaction region in the main linac and for power transfer efficiency in the drive linac. Thus they have to be isochronous. A preliminary study of them has been carried out at the first order using the tools described in the previous section. The results are summarized in Table 2 and Figs 3 and 4.

The less stringent constraint on the horizontal emittance growth for the drive beam allows one to obtain a smaller arc radius than could be expected from the energy scaling alone. Thus larger horizontal emittance growth would be acceptable but difficult to achieve due to limitations in optics matching.

On the contrary for the main beam the fractional horizontal emittance growth ($> 74\%$) cannot be further relaxed to obtain smaller arc radius because it would induce a significant loss of luminosity.

VI. DISCUSSION

This report shows the existence of a parametrized family of isochronous arcs and analytical procedures to design them. Simple interactive programming tools have been developed to implement these procedures which speed up the search of near optimized isochronous arcs. The first-order anisochronism is fully eliminated and the low values of the dispersion contribute to the second-order effects as well as to limiting the horizontal emittance growth. On the other hand, this makes the correction of the chromaticity with sextupoles more difficult because they cannot be placed where the dispersion is sufficiently high. This however becomes a severe problem when the arc is part of a ring through which the beam passes several times. Further investigations will be aimed at limiting these effects and studying the energy spread acceptance of such arcs. Trackings should provide results on the behaviour of this family of isochronous arcs at high orders.

Table 2: Parameters of the 360-degree isochronous arcs

| Parameter | 3 GeV arc | 9 GeV arc |
|---------------------------------|--------------------|--------------------|
| Number of insertions | 3 | 48 |
| Length of bending magnet | 1.8 m | 1 m |
| Quadrupole length | 0.3 m | 0.5 m |
| Gradient of the focusing quad | 55 T/m | 60 T/m |
| Gradient of the defocusing quad | 55 T/m | 60 T/m |
| L ₁ | 1.366 m | 2.068 m |
| L ₂ | 0.227 m | 0.925 m |
| L ₃ | 1.164 m | 0.310 m |
| Overall arc diameter | 15 m | 214 m |
| Horizontal phase advance | .../2 | .../2 |
| Vertical phase advance | .../3 | .../3 |
| Nominal ϕ_x (mrad) | 5×10^4 | 2.5×10^6 |
| $\phi \circ \phi_x$ (mrad) | 8.16×10^6 | 1.84×10^7 |

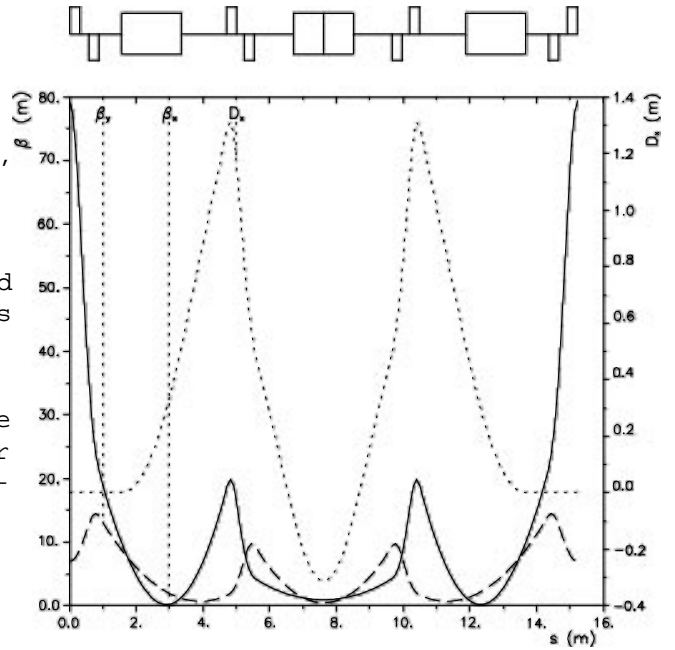


Figure 3: Optics functions of the 3 GeV isochronous module.

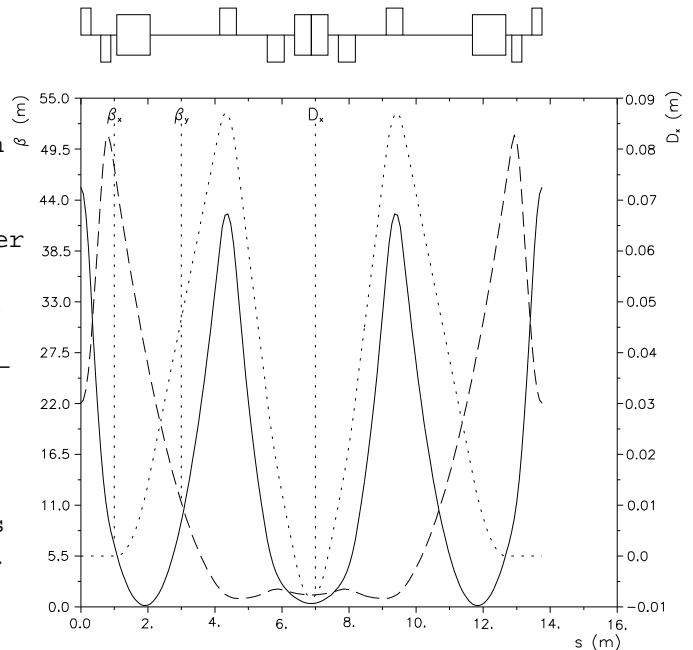


Figure 4: Optics functions of the 9 GeV isochronous module.

VII. REFERENCES

- [1] K.G. Steffen High Energy Beam Optics New York: Interscience 1965.
- [2] G. Guignard A Lattice with no Transition and Large Dynamic Aperture in Proc. 13th Particle Acceleration Conference Chicago 1989.
- [3] CEBAF Design Report May 1986.
- [4] E.T. d'Amico and G. Guignard CLIC note (in preparation).